

# Histamine Induces ATP Release from Human Subcutaneous Fibroblasts, via Pannexin-1 Hemichannels, Leading to $\text{Ca}^{2+}$ Mobilization and Cell Proliferation\*

Ana Rita Pinheiro<sup>‡§1</sup>, Diogo Paramos-de-Carvalho<sup>‡</sup>, Mariana Certal<sup>‡</sup>, Maria Adelina Costa<sup>‡¶</sup>, Cristina Costa<sup>‡</sup>, Maria Teresa Magalhães-Cardoso<sup>‡</sup>, Fátima Ferreirinha<sup>‡</sup>, Jean Sévigny<sup>||\*\*2</sup>, and Paulo Correia-de-Sá<sup>‡3</sup>

From the <sup>‡</sup>Laboratório de Farmacologia e Neurobiologia, Unidade Multidisciplinar de Investigação Biomédica (UMIB), and the <sup>¶</sup>Departamento de Química, Instituto de Ciências Biomédicas Abel Salazar-Universidade do Porto (ICBAS-UP), 4050-313 Porto, Portugal, the <sup>§</sup>Área Técnico-Científica de Fisioterapia, Escola Superior de Tecnologia da Saúde do Instituto Politécnico do Porto, 4400-330 Vila Nova de Gaia, Portugal, the <sup>||</sup>Centre de Recherche en Rhumatologie et Immunologie, Centre Hospitalier Universitaire de Québec, Québec, Québec G1V 4G2, Canada, and the <sup>\*\*</sup>Département de Microbiologie-Infectiologie et d'Immunologie, Faculté de Médecine, Université Laval, Québec, Québec G1V 0A6, Canada

**Background:** Chronic pain may involve connective tissue remodeling due to inflammatory mediators.

**Results:** Histamine  $\text{H}_1$  receptor activation causes ATP release from human subcutaneous fibroblasts via pannexin-1 hemichannels.

**Conclusion:** Responses of skin fibroblasts to histamine are amplified by autocrine ATP release and  $\text{P2Y}_1$  purinoceptor activation.

**Significance:** Amplification of histamine-mediated  $\text{Ca}^{2+}$  mobilization and growth of human fibroblasts by purines may be a novel therapeutic target for painful fibrotic diseases.

Changes in the regulation of connective tissue ATP-mediated mechano-transduction and remodeling may be an important link to the pathogenesis of chronic pain. It has been demonstrated that mast cell-derived histamine plays an important role in painful fibrotic diseases. Here we analyzed the involvement of ATP in the response of human subcutaneous fibroblasts to histamine. Acute histamine application caused a rise in intracellular  $\text{Ca}^{2+}$  ( $[\text{Ca}^{2+}]_i$ ) and ATP release from human subcutaneous fibroblasts via  $\text{H}_1$  receptor activation. Histamine-induced  $[\text{Ca}^{2+}]_i$  rise was partially attenuated by apyrase, an enzyme that inactivates extracellular ATP, and by blocking  $\text{P2}$  purinoceptors with pyridoxal phosphate-6-azo(benzene-2,4-disulfonic acid) tetrasodium salt and reactive blue 2.  $[\text{Ca}^{2+}]_i$  accumulation caused by histamine was also reduced upon blocking pannexin-1 hemichannels with  $^{10}\text{Panx}$ , probenecid, or carbenoxolone but not when connexin hemichannels were inhibited with mefloquine or 2-octanol. Brefeldin A, an inhibitor of vesicular exocytosis, also did not block histamine-induced  $[\text{Ca}^{2+}]_i$  mobilization. Prolonged exposure of human subcutaneous fibroblast cultures to histamine favored cell growth and type I collagen synthesis via the activation of  $\text{H}_1$  receptor. This effect was mimicked by ATP and its metabolite, ADP, whereas the selective  $\text{P2Y}_1$  receptor antagonist, MRS2179, partially attenuated histamine-induced cell growth and type I collagen production. Expression of pannexin-1 and ADP-sensitive  $\text{P2Y}_1$  receptor on human subcutaneous fibroblasts was confirmed by immunofluorescence confocal microscopy and Western blot analysis. In conclusion, histamine induces ATP release from human subcutaneous fibroblasts, via pannexin-1 hemichannels, leading to  $[\text{Ca}^{2+}]_i$  mobilization and cell growth through the cooperation of  $\text{H}_1$  and  $\text{P2}$  (probably  $\text{P2Y}_1$ ) receptors.

Unspecialized connective tissue forms an anatomical mesh throughout the body, which acts as a body-wide mechanosensitive signaling network (1, 2). Despite its overwhelming size, the relative importance of unspecialized connective tissue has been generally overlooked or misunderstood; it was considered as relatively superfluous apart from its supporting role among more specialized tissues (2). Nowadays, evidence suggests that increased connective tissue disorganization may be an important link in the pathogenesis of chronic musculoskeletal pain, such as low back pain (3, 4), and we hypothesized that this might also occur in fibromyalgia.

Like the skin, the underlying subcutaneous connective tissue is richly innervated by sensory nerve endings, including mechanoreceptors, nociceptors, and thermoreceptors (5, 6). Therefore, sensory inputs arising from affected connective tissue may alter the activity of nociceptors. Conversely, activation of nociceptors causes the release of substance P from sensory C-fibers, which triggers the production of inflammatory mediators, like histamine and several cytokines, from neighboring cells (7). It was demonstrated that substance P and histamine augment

cytokine-induced proliferation of dermal fibroblasts, thus indicating that mast cell-derived histamine may be a key player in the induction of tissue fibrosis in painful fibrotic diseases (8). In view of this, nociceptor activation may by itself contribute to prolong inflammation and to exaggerate tissue fibrosis.

Inflammatory mediators, such as cytokines and histamine, are essential to the onset and maintenance of inflammatory reactions (9). In addition, adenine and uracil nucleotides have also been related to the pathophysiology of chronic inflammation (10). Besides their acute actions, nucleotides exert autocrine and/or paracrine activities regulating cellular processes like proliferation and differentiation of human cells (11). Interestingly, it has been described that smooth muscle and epithelial cells release ATP in response to histamine (12), but this was never demonstrated in fibroblasts. Therefore, we postulated that inflammatory mediators, like histamine, could influence connective tissue plasticity through the release of ATP from fibroblasts, the predominant cell type of this tissue, leading to signal amplification via P2 purinoceptors located in neighboring cells.

Nucleotides reach the external milieu via both lytic and non-lytic mechanisms from various cell types upon mechanical or chemical stimulation. Nucleotide-releasing pathways include 1) electrodiffusional movement through membrane ion channels, including pannexin and connexin hemichannels; 2) facilitated diffusion by nucleotide-specific ATP-binding cassette transporters; and 3) cargo vesicle trafficking and exocytotic granule secretion (13). The extent of the paracrine activity mediated by ATP and/or related released nucleotides may be limited by the presence of membrane-bound nucleotide-metabolizing enzymes. Ectonucleotidases sequentially catabolize nucleoside 5'-triphosphates to their respective nucleoside 5'-di- and monophosphates, nucleosides, and free phosphates or pyrophosphate, which can all appear in the extracellular fluid at the same time (13). Although a comprehensive study on the kinetics of extracellular catabolism of adenine nucleotides and adenosine formation in the human musculoskeletal system is still lacking, the coexistence of various metabolic pathways for the nucleotide extracellular hydrolysis represents an opportunity for regulating cell-specific responses to surrounding adenine nucleotides and for terminating purinergic actions.

Therefore, this study was designed to investigate if the response of human subcutaneous fibroblasts to histamine involves a purinergic loop consisting in the release of ATP, formation of its biological active metabolites (namely ADP), and subsequent activation of P2 purinoceptors. Understanding the mechanisms underlying the purinergic amplification loop regulating cell signaling and subcutaneous tissue remodeling triggered by inflammatory mediators may highlight new therapeutic strategies for chronic painful conditions.

## EXPERIMENTAL PROCEDURES

**Materials and Reagents**—Materials and reagents are described in detail in the [supplemental Experimental Procedures](#).

**Cell Cultures**—Human fibroblasts were isolated from the subcutaneous tissue of organ donors ( $52 \pm 5$  years old (means  $\pm$  S.E. of the mean),  $n = 16$ ) with no clinical history of connective tissue disorders. The protocol was approved by the

Ethics Committee of Hospital Geral de Santo António SA (University Hospital) and of the Instituto de Ciências Biomédicas de Abel Salazar (Medical School) of the University of Porto. The investigation conforms to the principles outlined in the Declaration of Helsinki. Subcutaneous tissues were maintained at  $4-6^{\circ}\text{C}$  in M-400 transplantation solution (4.190 g/100 ml mannitol, 0.205 g/100 ml  $\text{KH}_2\text{PO}_4$ , 0.970 g/100 ml  $\text{K}_2\text{HPO}_4 \cdot 3\text{H}_2\text{O}$ , 0.112 g/100 ml KCl, and 0.084 g/100 ml  $\text{NaHCO}_3$ , pH 7.4) until used, which was between 2 and 16 h after being harvested (14). Cells were then obtained by the explant technique and cultured in DMEM supplemented with 10% fetal bovine serum (FBS),  $2.5 \mu\text{g}/\text{ml}$  amphotericin B, and 100 units/ml penicillin/streptomycin at  $37^{\circ}\text{C}$  in a humidified atmosphere of 95% air and 5%  $\text{CO}_2$ . Medium was replaced twice a week. Primary cultures were maintained until near confluence ( $\sim 3-4$  weeks), and then adherent cells were enzymatically released with 0.04% trypsin-EDTA solution plus 0.025% type I collagenase in phosphate-buffered saline (PBS). The resultant cell suspension was cultured and maintained in the same conditions mentioned above. All of the experiments were performed in the first subculture.

**Extracellular ATP Quantification by Bioluminescence**—Extracellular ATP was quantified by the luciferin-luciferase ATP bioluminescence assay kit HS II (Roche Applied Science), using a multidetection microplate reader (Synergy HT, BioTek Instruments). Briefly, cells were seeded in flat bottom 96-well plates at a density of  $3 \times 10^4$  cells/ml for 21 days. At the beginning of the experiment, cells were washed twice with Tyrode's solution (137 mM NaCl, 2.7 mM KCl, 1.8 mM  $\text{CaCl}_2$ , 1 mM  $\text{MgCl}_2$ , 0.4 mM  $\text{NaH}_2\text{PO}_4$ , 11.9 mM  $\text{NaHCO}_3$ , and 11.2 mM glucose, pH 7.4) at  $37^{\circ}\text{C}$  and allowed to rest for 30 min (basal), after which samples were collected ( $75 \mu\text{l}$ ). Subsequently, histamine ( $100 \mu\text{M}$ ) was added. Samples were collected at five different incubation times (0–240 s) and immediately stored at  $-20^{\circ}\text{C}$ . Luciferin-luciferase experiments were performed at room temperature, and light emission acquisition was performed 20 s after the addition of luciferin-luciferase to the collected sample.

**Measurement of  $[\text{Ca}^{2+}]_i$** —Changes in  $[\text{Ca}^{2+}]_i$  were measured with the calcium-sensitive dye Fluo-4 NW using the multidetection microplate reader referred to above (15). Human fibroblasts were seeded in flat bottom 96-well plates at a density of  $3 \times 10^4$  cells/ml. Cells were cultured for 5–15 days in supplemented DMEM as described above. On the day of the experiment, cells were washed twice with Tyrode's solution and incubated at  $37^{\circ}\text{C}$  for 45 min with the cell-permeant fluorescent  $\text{Ca}^{2+}$  indicator, Fluo-4 NW ( $2.5 \mu\text{M}$ ). After removal of the fluo-4 loading solution, cells were washed again twice, and 150/300  $\mu\text{l}$  of Tyrode's solution was added per culture well/dish, respectively. For the recordings, temperature was maintained at  $32^{\circ}\text{C}$ , and readings were carried out during  $\sim 30$  min each every 5 s, using a tungsten halogen lamp. Fluorescence was excited at 485/20 nm, and emission was measured at 528/20 nm. Calcium measurements were calibrated to the maximal calcium load produced by ionomycin ( $5 \mu\text{M}$ ; 100% response) (16, 17).

**Single-cell  $[\text{Ca}^{2+}]_i$  Imaging and To-Pro3 Dye Uptake Detection by Confocal Microscopy**—In some of the experiments, we monitored single-cell  $[\text{Ca}^{2+}]_i$  oscillations and To-Pro3 dye uptake from the same cells by confocal microscopy (FV1000,

Olympus, Japan) (11). Due to their high molecular mass, carbo-cyanine monomer nucleic acid fluorescent dyes, like To-Pro3 (671 Da), are membrane-impermeable and are generally excluded from viable cells unless large diameter pores open. Thus, increases in fluorescence intensity can be taken as measure of To-Pro3 dye uptake into viable cells, which may occur through connexin and pannexin-1 hemichannels that conduct molecules up to 1 kDa in size across the plasma membrane (ATP is 507 Da). Human subcutaneous fibroblasts were seeded onto 35-mm glass bottom dishes at a density of  $2 \times 10^4$  cells/ml and allowed to grow for 5–15 days in supplemented DMEM, as described above. On the day of the experiment, cells were first loaded with the fluorescent  $\text{Ca}^{2+}$  indicator, Fluo-4 NW ( $2.5 \mu\text{M}$ ; see above). Culture dishes were mounted on a thermostatic ( $32^\circ\text{C}$ ) perfusion chamber at the stage of an inverted laser-scanning confocal microscope equipped with a  $\times 20$  magnification objective lens (LUCPLFLN  $\times 20$  PH; numerical aperture, 0.45). The chamber was continuously superfused (1 ml/min) with gassed (95%  $\text{O}_2$ , 5%  $\text{CO}_2$ , pH 7.4) Tyrode's solution. To monitor histamine-induced hemichannels opening in parallel to  $[\text{Ca}^{2+}]_i$  oscillations, To-Pro3 iodide ( $1 \mu\text{M}$ ) was added to the superfusion solution 6 min before histamine application and was kept up to the end of the experiment. Fluo-4 NW was excited with a 488-nm multiline argon laser, and the emitted fluorescence was detected at 510–560 nm; TO-PRO-3 was excited with a 633-nm red helium-neon laser, and the emitted fluorescence was detected at 661 nm. Time-lapse sequences were recorded at scanning rates with a 20-s interval for  $\sim 30$  min, digitized, and processed off-line. Regions of interest were defined manually.

**Cell Viability/Proliferation**—Viability/proliferation studies included the 3-[4,5-dimethylthiazol-2-yl]-2,5-diphenyltetrazolium bromide (MTT)<sup>4</sup> assay as described previously (18). Human fibroblasts were seeded in flat bottom 96-well plates at a density of  $3 \times 10^4$  cells/ml and cultured in supplemented DMEM as described above. Cell cultures were routinely monitored by phase-contrast microscopy and characterized at days 1, 7, 14, 21, and 28. The MTT assay consists of the reduction of MTT to a purple formazan reaction product by viable cells. In the last 4 h of each test period, cells were incubated with 0.5 mg/ml MTT for 4 h in the conditions described above. The medium was carefully removed and decanted, and the stained product was dissolved with DMSO before absorbance (A)

determination at 600 nm using a microplate reader spectrometer. Results were expressed as A/well.

**Total Type I Collagen Determination**—Type I collagen determination was performed using the Sirius Red staining assay. Human fibroblasts were cultured as described for the viability/proliferation studies. The staining protocol was adapted from Tulberg-Reinert and Jundt (19). Cell layers were washed twice in PBS before fixation with Bouin's fluid for 1 h. The fixation fluid was removed by suction, and the culture plates were washed by immersion in running tap water for 15 min. Culture dishes were allowed to air-dry before adding the Sirius Red dye (Direct Red 80). Cells were stained for 1 h under mild shaking on a microplate shaker. To remove non-bound dye, stained cells were washed with 0.01 N hydrochloric acid and then dissolved in 0.1 N sodium hydroxide for 30 min at room temperature using a microplate shaker. Optical density was measured at 550 nm against 0.1 N sodium hydroxide as a blank (19). Results were expressed as A/well.

**Enzymatic Kinetic Experiments and HPLC Analysis**—After a 30-min equilibration period at  $37^\circ\text{C}$ , culture day 11 cells were incubated with 30  $\mu\text{M}$  ATP, ADP, or AMP, which was added to the culture medium at zero time. Samples (75  $\mu\text{l}$ ) were collected from each well at different times up to 30 min for high performance liquid chromatography (HPLC) (LaChrome Elite, Merck) analysis of the variation of substrate disappearance and product formation (11, 20). ATP and ADP catabolism analysis was performed by ion pair reverse-phase HPLC (21), whereas AMP catabolism analysis used a linear gradient (100% 100 mM  $\text{KH}_2\text{PO}_4$ , pH 7, to 100% 100 mM  $\text{KH}_2\text{PO}_4$ , pH 7, 30% methanol) for 10 min with a constant rate flow of 1.25 ml/min. Under these conditions, the retention times of metabolites were as follows: AMP (2.17 min), hypoxanthine (3.07 min), inosine (5.09 min), and adenosine (7.51 min). Concentrations of the substrate and products were plotted as a function of time (progress curves). The following parameters were analyzed for each progress curve: half-life time ( $t_{1/2}$ ) of the initial substrate, time of appearance of the different concentrations of the products, and concentration of the substrate or any product remaining at the end of the experiment.

The spontaneous degradation of adenine nucleotides and nucleosides at  $37^\circ\text{C}$  in the absence of the cells was negligible (0–3%) over 30 min. At the end of the experiments, the remaining incubation medium was collected and used to quantify the lactate dehydrogenase (EC 1.1.1.27) activity. The negligible activity of lactate dehydrogenase in the samples collected at the end of the experiments is an indication of the integrity of the cells during the experimental period.

**Antibody Production**—The development and specificity of anti-human nucleoside triphosphate diphosphohydrolase 2 (NTPDase2) and NTPDase3 has been reported previously (22, 23). Hartley guinea pigs and New Zealand rabbits were obtained from Charles River Laboratories (Québec, Canada). The genetic immunization protocol was carried out with plasmids (pcDNA3 for human NTPDase1 and pcDNA3.1 for human CD73) encoding each protein using New Zealand rabbits for antibodies against human NTPDase1 and Hartley guinea pigs for human CD73 antibodies.

<sup>4</sup> The abbreviations and trivial names used are: MTT, thiazolyl blue formazan, 1-(4,5-dimethylthiazol-2-yl)-3,5-diphenylformazan; AR-C 66096, 2-(propylthio)adenosine-5'-O-( $\beta$ , $\gamma$ -difluoromethylene)triphosphate tetrasodium salt; ATP $\gamma$ S, adenosine 5'-[ $\gamma$ -thio]triphosphate tetralithium salt; BFA, brefeldin A; CBX, carbenoxolone; Cx, connexin; NTPDase, nucleoside triphosphate diphosphohydrolase; E-NTPDase, ecto-nucleoside triphosphate diphosphohydrolase; H1152, (S)-(+)-2-methyl-1-((4-methyl-5-isoquinolyl)sulfonyl)-hexahydro-1H-1,4-diazepine dihydrochloride; Hist, histamine; MFQ, mefloquine; MRS 2179, 2'-deoxy-N<sup>6</sup>-methyladenosine 3',5'-bisphosphate tetrasodium salt; MRS 2211, 2-((2-chloro-5-nitrophenyl)azo)-5-hydroxy-6-methyl-3-((phosphonoxy)methyl)-4-pyridinecarboxaldehyde disodium salt; Panx, pannexin; PPADS, 4-((4-formyl-5-hydroxyl-6-methyl-3-((phosphonoxy)methyl)-2-pyridinyl)azo)-1,3-benzenedisulfonic acid tetrasodium salt; RB-2, reactive blue 2; TNP-ATP, 2',3'-O-(2,4,6-trinitrophenyl)adenosine-5'-triphosphate tetra(triethylammonium) salt; U73122, 1-(6-(((17 $\beta$ )-3-methoxyestra-1,3,5(10)-trien-17-yl)amino)hexyl)-1H-pyrrole-2,5-dione.



**Immunocytochemistry**—Human fibroblasts were seeded in chamber slides at a density of  $2.5 \times 10^4$  cells/ml and allowed to grow for 5–15 days. Cultured cells were fixed in 4% paraformaldehyde in PBS for 10 min, washed three times in PBS (10 min each), and subsequently, incubated with blocking buffer I (10% FBS, 1% bovine serum albumin (BSA), 0.1% Triton X, 0.05%  $\text{NaN}_3$ ) for 1 h. Primary antibodies, diluted in blocking buffer II (5% FBS, 1% BSA, 0.1% Triton X, 0.05%  $\text{NaN}_3$ ), were applied (mouse anti-porcine vimentin (1:75) (DAKO, Denmark); rabbit anti-human collagen I (1:50) (AbDSerotec); rabbit anti-human P2Y<sub>1</sub> (1:50), rabbit anti-human P2Y<sub>12</sub> (1:100), and rabbit anti-human P2Y<sub>13</sub> (1:25) (Alomone); rabbit anti-human Cx43 (1:600) and rabbit anti-human pannexin 1 (Pannx1) (1:1000) (Abcam); and rabbit anti-human NTPDase1 (1:100), rabbit anti-human NTPDase2 (1:200), mouse anti-human NTPDase3 (1:200), and guinea pig anti-human CD73 (1:300) (University of Laval, Québec, Canada); see the Centre de Recherche du CHUL Web site for further details), and the slides were incubated overnight at 4 °C. After incubation, cells were washed three times in 1× PBS (10 min each). The donkey anti-rabbit IgG Alexa Fluor 488, donkey anti-mouse IgG Alexa Fluor 488, donkey anti-mouse IgG Alexa Fluor 568, and donkey anti-guinea pig IgG Alexa Fluor 568 secondary antibodies (Invitrogen) were diluted in blocking buffer II (5% FBS, 1% BSA, 0.1% Triton X) and applied for 1 h in the dark. A last wash was performed with 1× PBS, and glass slides were mounted with VectaShield medium and stored at 4 °C. Observations were performed and analyzed with an Olympus FV1000 confocal microscope (11, 24).

**SDS-PAGE and Western Blotting**—Fibroblasts were homogenized in a lysis buffer with the following composition: 50 mM Tris-HCl (pH 8.0), 150 mM NaCl, 0.5% sodium deoxycholate, 1% Triton X-100, 0.1% SDS, and a protease inhibitor mixture. Protein content of the samples was evaluated using the BCA protein assay kit according to the manufacturer's instructions (Pierce). Samples were solubilized in SDS reducing buffer (0.125 mM Tris-HCl, 4% SDS, 0.004% bromophenol blue, 20% glycerol, and 10% 2-mercaptoethanol, pH 6.8, at 70 °C for 10 min), subjected to electrophoresis in 10% SDS-polyacrylamide gels, and electrotransferred onto PVDF membranes (MilliPore, MA). Protein loads were 60 µg for P2Y<sub>1</sub>, P2Y<sub>12</sub>, and P2Y<sub>13</sub>, 25 µg for Pannx1, and 15 µg for Cx43. The membranes were blocked for 1 h in Tris-buffered saline (TBS; 10 mM Tris-HCl, pH 7.5, 150 mM NaCl) containing 0.05% Tween 20 + 5% BSA. Membranes were subsequently incubated with goat anti-human P2Y<sub>1</sub> (1:200) (Santa Cruz Biotechnology, Inc.), rabbit anti-human P2Y<sub>12</sub> (1:200) (Alomone), rabbit anti-human P2Y<sub>13</sub> (1:200) (Alomone), rabbit anti-human Pannx1 (1:250) (Novex, Invitrogen), and rabbit anti-human Cx43 (1:6000) (Abcam) in the above blocking buffer overnight at 4 °C. Membranes were washed three times for 10 min in 0.1% Tween 20 in TBS and then incubated with donkey anti-rabbit IgG (HRP) (1:30,000) (Abcam) and donkey anti-goat IgG (HRP) (1:25,000) (Abcam) secondary antibodies for 60 min at room temperature. For comparison purposes, the membranes were also incubated with rabbit anti-human  $\beta$ -tubulin (1:2500) (Abcam) antibody following the procedures described above. Membranes were washed three times for 10 min, and antigen-antibody com-

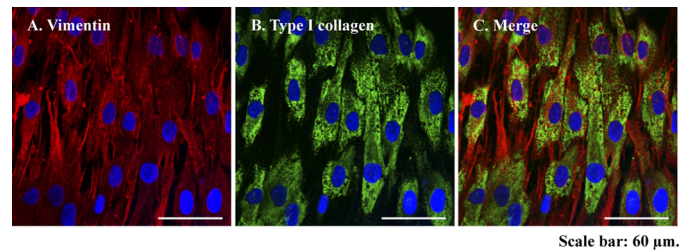


**FIGURE 1. Immunocytochemistry staining of fibroblasts isolated from human subcutaneous tissue.** Cells exhibited positive immunoreactivity against vimentin, which has been described as a reliable fibroblast marker (red) (A). Most of the cells also stained positive to type I collagen (green) (B), which is highly produced by activated fibroblasts. C, merge of vimentin and type I collagen staining. Scale bar, 60 µm.

plexes were visualized by chemiluminescence with an ECL reagent using the ChemiDoc MP imaging system (Bio-Rad).

**Presentation of Data and Statistical Analysis**—Data are expressed as mean  $\pm$  S.E. from  $n$  number of experiments/cells/individuals. Data from different individuals were evaluated by one-way analysis of variance. Statistical differences found between control and drug-treated cultures were determined by Bonferroni's method.  $p$  values of  $<0.05$  were considered to represent significant differences.

## RESULTS

**Fibroblast Characterization**—Cultured cells were elongated and showed a spindle-shaped morphology that is characteristic of fibroblasts (25, 26). Their fibroblastic nature was confirmed by immunocytochemistry. All cells exhibited a positive immunoreactivity against vimentin, the intermediate protein filament considered a reliable fibroblast cell marker (Fig. 1A) (27). Cells also stained positive for type I collagen (Fig. 1B), which is highly produced by fibroblasts (27).

**Histamine Recruits  $\text{Ca}^{2+}$  from Intracellular Stores via the Activation of  $\text{H}_1$  Receptors Coupled to Phospholipase C**—Incubation of human subcutaneous fibroblasts with histamine (100 µM,  $n = 34$ ) caused a fast (within seconds) rise in  $[\text{Ca}^{2+}]_i$ , which attained  $35 \pm 2\%$  of the maximal calcium load produced by ionomycin (5 µM; 100% response) (Fig. 2B). Although the kinetics of  $[\text{Ca}^{2+}]_i$  rise induced by histamine differed slightly among cells (see Fig. 2B, iv), the initial fast phase was always followed by a slow decay lasting about 2 min; beyond that point,  $[\text{Ca}^{2+}]_i$  levels remained fairly constant until drug washout (Fig. 2B, iii).

Histamine-induced  $[\text{Ca}^{2+}]_i$  oscillations were significantly ( $p < 0.05$ ) attenuated by selective blockade of  $\text{H}_1$  receptors with cetirizine, applied in a concentration (1 µM,  $n = 6$ ) that on its own did not change base line (Fig. 2C). Phospholipase C involvement in histamine-induced  $[\text{Ca}^{2+}]_i$  response was confirmed using the phospholipase C inhibitor U73122 (3 µM,  $n = 6$ ) (Fig. 2D).  $[\text{Ca}^{2+}]_i$  oscillations produced by histamine (100 µM,  $n = 10$ ) were also prevented ( $p < 0.05$ ) by the selective inhibitor of endoplasmic reticulum  $\text{Ca}^{2+}$ -ATPase, thapsigargin (2 µM,  $n = 4$ ), which is known to deplete intracellular  $\text{Ca}^{2+}$  stores following a transient ( $<2$ -min) rise of  $[\text{Ca}^{2+}]_i$  levels (28) (Fig. 2E). The removal of external  $\text{Ca}^{2+}$  ( $\text{Ca}^{2+}$ -free medium plus EGTA; 100 µM,  $n = 4$ ) depressed ( $p < 0.05$ ) only the late component of histamine (100 µM,  $n = 13$ ) response, keeping constant the initial fast rise (Fig. 2F).

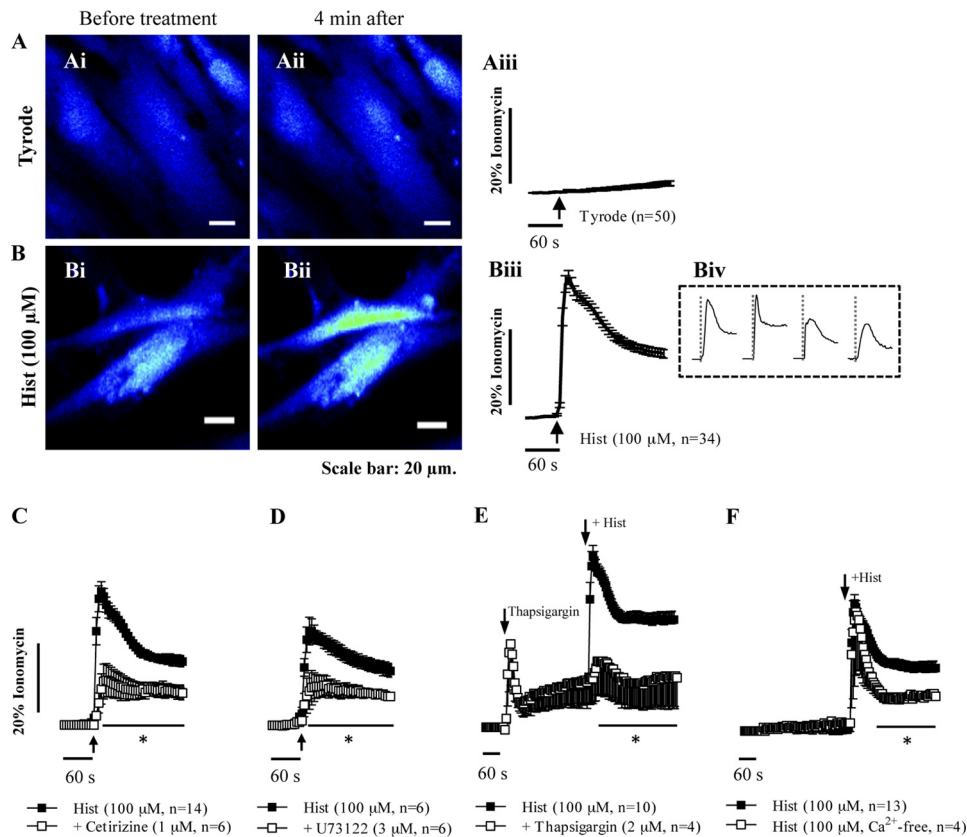


**FIGURE 2. Histamine recruits  $\text{Ca}^{2+}$  from intracellular stores via the activation of  $\text{H}_1$  receptors.** A and B, fluorescence  $[\text{Ca}^{2+}]_i$  oscillations in human subcutaneous fibroblasts in culture in the absence (A) and in the presence (B) of histamine (Hist) (100  $\mu\text{M}$ ). Cells were preincubated with the fluorescent calcium indicator Fluo-4 NW; changes in fluorescence were detected in the time-lapse mode using a confocal microscope (A (i and ii) and B (i and ii)) or a microplate reader (A (iii) and B (iii)) (see “Experimental Procedures”). Note that the kinetics of  $[\text{Ca}^{2+}]_i$  signals produced by histamine differed slightly among cells (B, iv).  $[\text{Ca}^{2+}]_i$  transients were calibrated to the maximal calcium load produced by ionomycin (5  $\mu\text{M}$ ; 100% response). Shown are also  $[\text{Ca}^{2+}]_i$  oscillations produced by Hist (100  $\mu\text{M}$ ) applied in the presence of the selective  $\text{H}_1$  receptor antagonist cetirizine (1  $\mu\text{M}$ ; C), the phospholipase C inhibitor U73122 (3  $\mu\text{M}$ ; D), and the selective endoplasmic reticulum  $\text{Ca}^{2+}$ -ATPase inhibitor thapsigargin (2  $\mu\text{M}$ ; E) and after removal of extracellular  $\text{Ca}^{2+}$  ( $\text{Ca}^{2+}$ -free medium plus EGTA, 100  $\mu\text{M}$ ; F). Black arrows, time of drug application. Each point represents pooled data from  $n$  experiments. Vertical bars, S.E., shown when they exceed the symbols in size. Image scale bars, 20  $\mu\text{m}$ . \*,  $p < 0.05$ , significant differences from Hist (100  $\mu\text{M}$ ) alone.

**Histamine-induced  $[\text{Ca}^{2+}]_i$  Accumulation Is Partially Dependent on ATP Release, Leading to P2 Purinoceptor Activation**—Using the luciferin-luciferase bioluminescence assay, results show that histamine (100  $\mu\text{M}$ ) significantly ( $p < 0.05$ ) increased ATP release from human subcutaneous fibroblasts as compared with the control situation where the cells were exposed to Tyrode’s solution (Fig. 3A).

Extracellular ATP inactivation with apyrase (2 units/ml,  $n = 9$ ) reduced significantly ( $p < 0.05$ ) the late component of histamine (100  $\mu\text{M}$ ,  $n = 26$ ) response while keeping fairly conserved the magnitude of the initial  $[\text{Ca}^{2+}]_i$  rise (Fig. 3B, i). A similar pattern was observed when human subcutaneous fibroblasts were preincubated with non-selective P2 antagonists, RB-2 (100  $\mu\text{M}$ ,  $n = 7$ ) and PPADS (100  $\mu\text{M}$ ,  $n = 6$ ) (Fig. 3B, ii and iii, respectively). Attenuation of histamine-induced  $[\text{Ca}^{2+}]_i$  oscillations by PPADS and RB-2 ( $p < 0.05$ ) contrasts with the absence of effect obtained with the preferential P2X receptor antagonist, TNP-ATP (10  $\mu\text{M}$ ,  $n = 2$ ) (data not shown).

In line with these observations, exogenous application of ATP and ADP (0.1–1 mM) concentration-dependently increased  $[\text{Ca}^{2+}]_i$ ; when applied at a 1 mM concentration, ATP and ADP transiently increased  $[\text{Ca}^{2+}]_i$ , reaching  $43 \pm 4\%$  ( $n =$

26) and  $25 \pm 8\%$  ( $n = 3$ ), respectively, of the maximal calcium load caused by ionomycin within 20 s from drug application. ATP-induced  $[\text{Ca}^{2+}]_i$  transients were prevented ( $p < 0.05$ ) by preincubation of human subcutaneous fibroblasts with PPADS (300  $\mu\text{M}$ ) (Fig. 3B, iv).

**Histamine-induced  $[\text{Ca}^{2+}]_i$  Mobilization Depends on Pannexin-1 Hemichannel Activity**—Given that histamine-induced  $[\text{Ca}^{2+}]_i$  oscillations in human subcutaneous fibroblasts depend, at least partially, on the release of ATP and subsequent P2 purinoceptor activation, we tested the action of selective inhibitors of nucleotide-releasing pathways on histamine  $[\text{Ca}^{2+}]_i$  responses.

Cx43 expression is characteristic of fibroblasts from other tissue origins (1, 29), and connexin-containing hemichannels are putative mediators of ATP translocation into the extracellular milieu. Inhibition of connexin hemichannels, either with mefloquine (MFQ; 3  $\mu\text{M}$ ,  $n = 4$ ), which has been described as completely blocking Cx36- and Cx50-containing hemichannels (30, 31), or with 2-octanol (1 mM,  $n = 7$ ), which blocks Cx43, Cx46, and Cx50 hemichannels (31, 32), failed to modify ( $p > 0.05$ ) histamine-induced  $[\text{Ca}^{2+}]_i$  signals (Fig. 4A, i and ii, respectively). Despite the fact that 2-octanol (1 mM,  $n = 7$ ) failed to modify  $[\text{Ca}^{2+}]_i$  rises caused by histamine (100  $\mu\text{M}$ ), we

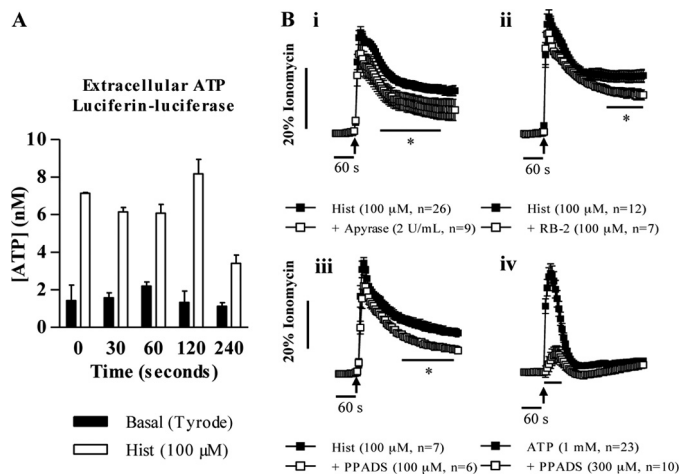


**FIGURE 3. Histamine-induced  $[Ca^{2+}]_i$  mobilization in cultured human subcutaneous fibroblasts is partially dependent on ATP release and P2 purinoceptors activation.** A, ATP content (nmol) of samples from the incubation medium in the presence of Hist (100  $\mu$ M) as compared with the control condition where only Tyrode's solution was applied (luciferin-luciferase ATP bioluminescence assay). Each bar represents pooled data from 2–3 replicates of one individual. The vertical bars represent S.E. B, the effect of Hist (100  $\mu$ M) after pretreatment of the cells with apyrase (2 units/ml) (i), which catabolizes ATP and ADP into AMP, and two P2 receptor antagonists, RB-2 (100  $\mu$ M) (ii) and PPADS (100  $\mu$ M) (iii). For comparison purposes, we also tested the effect of ATP (1 mM) (iv) on  $[Ca^{2+}]_i$  oscillations in the absence and in the presence of PPADS (300  $\mu$ M). Cells were preincubated with the fluorescent calcium indicator Fluo-4 NW (see "Experimental Procedures");  $[Ca^{2+}]_i$  transients were calibrated to the maximal calcium load produced by ionomycin (5  $\mu$ M; 100% response). Black arrows, time of drug application. No changes in base-line fluorescence were observed after application of apyrase and the two P2 purinoceptor antagonists. Each point represents pooled data from  $n$  experiments. Vertical bars, S.E., shown when they exceed the symbols in size. \*,  $p < 0.05$ , significant differences from Hist (100  $\mu$ M) or ATP (1 mM) alone.

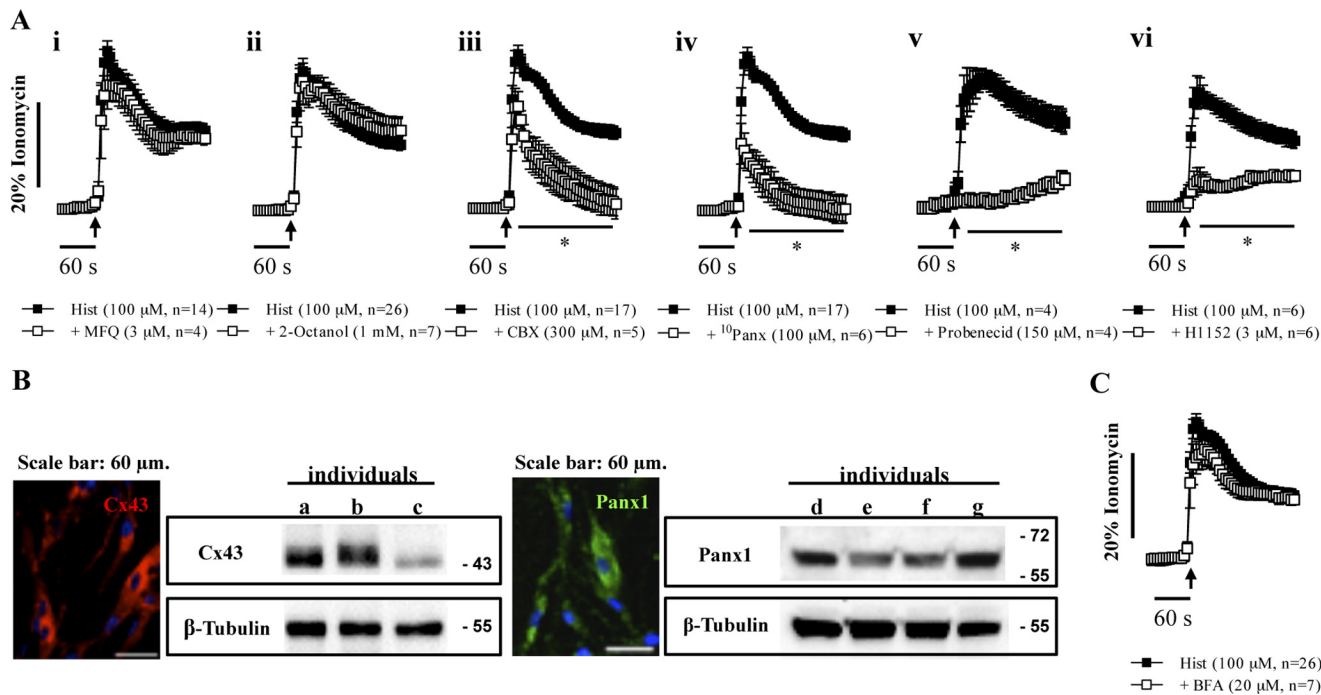


**FIGURE 4. Histamine-induced  $[Ca^{2+}]_i$  mobilization depends on pannexin-1 hemichannel activity in cultured human subcutaneous fibroblasts.** The effect of Hist (100  $\mu$ M) was tested in the presence of inhibitors of connexin- and/or pannexin-containing hemichannels, namely MFQ (3  $\mu$ M) (A, i), 2-octanol (1 mM) (A, ii), CBX (300  $\mu$ M) (A, iii),  $^{10}$ Panx (100  $\mu$ M) (A, iv), probenecid (150  $\mu$ M) (A, v), and H1152 (3  $\mu$ M) (A, vi) as well as upon blocking vesicle exocytosis with BFA (20  $\mu$ M) (C). Cells were preincubated with the fluorescent calcium indicator Fluo-4 NW (see "Experimental Procedures");  $[Ca^{2+}]_i$  transients were calibrated to the maximal calcium load produced by ionomycin (5  $\mu$ M; 100% response). Black arrows, time of drug application. None of the inhibitors significantly changed base-line fluorescence when applied alone. Each point represents pooled data from  $n$  experiments. Vertical bars, S.E., shown when they exceed the symbols in size. \*,  $p < 0.05$ , significant differences from Hist (100  $\mu$ M) alone. B, representative confocal micrographs and blots of Cx43 and Panx1 hemichannel immunoreactivity in cultured human subcutaneous fibroblasts from several distinct individuals (a–g).  $\beta$ -Tubulin was used as a reference protein. Image scale bars, 60  $\mu$ m.

re-evaluated the effect of MFQ, increasing its concentration to 30  $\mu$ M, which is high enough to completely block Cx43-containing hemichannels (31). Unfortunately, on its own, MFQ (30  $\mu$ M,  $n = 3$ ) produced an as yet unexplained rise ( $p < 0.05$ ) in  $[Ca^{2+}]_i$ , thus precluding further studies to test the histamine response (data not shown).

Carbenoxolone (CBX; 300  $\mu$ M,  $n = 5$ ), a non-selective inhibitor of connexins Cx26, Cx30, Cx32, Cx43, and Cx46, which also blocks Panx1-containing hemichannels (32), significantly ( $p < 0.05$ ) attenuated histamine-induced  $[Ca^{2+}]_i$  response (Fig. 4A, iii). The inhibitory effect of CBX (300  $\mu$ M) was reproduced by the selective Panx1 mimetic inhibitory peptide,  $^{10}$ Panx (100  $\mu$ M,  $n = 6$ ) (33) (Fig. 4A, iv), as well as by probenecid (150  $\mu$ M,  $n = 4$ ) (34), a powerful inhibitor of Panx1 hemichannels without any action on connexin-containing channels (Fig. 4A, v). Compounds that affect hemichannel pore permeability, like the Rho kinase inhibitor H1152 (3  $\mu$ M,  $n = 6$ ), also significantly ( $p < 0.05$ ) decreased histamine-induced  $[Ca^{2+}]_i$  rise (Fig. 4A, vi).

Using immunofluorescence confocal microscopy and Western blot analysis, we confirmed that fibroblasts of the human subcutaneous tissue in culture express both Cx43 and Panx1 (Fig. 4B). Despite this, data suggest that ATP release via Panx1 hemichannels play a more relevant role in histamine-evoked  $[Ca^{2+}]_i$  mobilization under the present experimental conditions.

The uptake of high molecular mass membrane-impermeable fluorescent dyes, such as To-Pro3, has been used to investigate hemichannels opening (leading to the release of ATP) in viable cells by time-lapse fluorescence microscopy (35). Data presented in Fig. 5 show that perfusion of cultured fibroblasts from



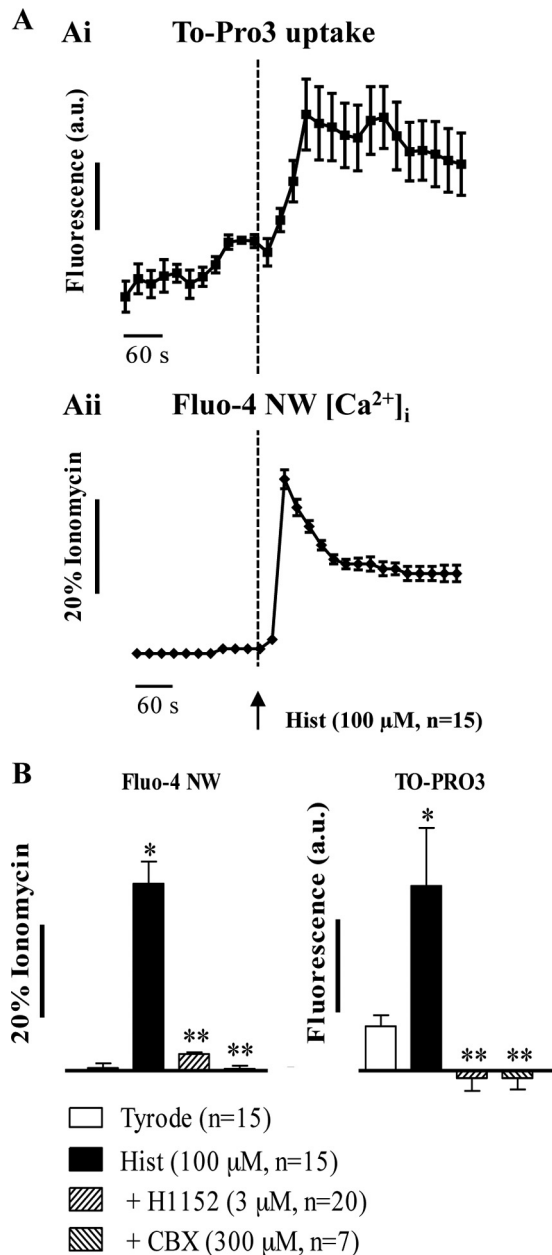


**FIGURE 5. Histamine-induced single-cell  $[Ca^{2+}]_i$  oscillations and To-Pro3 dye uptake by cultured fibroblasts of the human subcutaneous tissue evaluated by time-lapse fluorescence confocal microscopy.** *A*, fluorescence variation in cells preloaded with the fluorescent calcium indicator Fluo-4 NW (see "Experimental Procedures"); To-Pro3 was added to the superfusion fluid 6 min before Hist (100  $\mu$ M) (dashed vertical line). Results are in arbitrary units (a.u.) of fluorescence; individual  $[Ca^{2+}]_i$  transients were calibrated to the corresponding maximal calcium load produced by ionomycin (5  $\mu$ M; 100% response) in the same cell. *B*, bars represent the effect of Hist (100  $\mu$ M) in the absence and in the presence of pannexin-1 hemichannel permeability blockers, CBX (300  $\mu$ M) and H1152 (3  $\mu$ M). Vertical bars, S.E. from *n* experiments. \*,  $p < 0.05$ , significant differences from control values obtained in the absence of tested drugs; \*\*,  $p < 0.05$ , significant differences compared with the effect of Hist (100  $\mu$ M) alone.

the human subcutaneous tissue with histamine (100  $\mu$ M) caused a sustained rise of To-Pro3 dye uptake (Fig. 5*A*, *i*), which reached a maximum 30–40 s after the initial  $[Ca^{2+}]_i$  peak (Fig. 5*A*, *ii*). Compounds that block Panx1-containing channels, like CBX (300  $\mu$ M, *n* = 7), or affect hemichannel pore permeability, like H1152 (3  $\mu$ M, *n* = 20), significantly ( $p < 0.05$ ) decreased

histamine-induced  $[Ca^{2+}]_i$  rise and To-Pro3 dye uptake by human subcutaneous fibroblasts (Fig. 5*B*).

The involvement of nucleotide release by exocytosis was assessed using the vesicular transport inhibitor brefeldin A (BFA; 20  $\mu$ M). No statistically significant ( $p > 0.05$ ) differences were found in  $[Ca^{2+}]_i$  oscillations produced by histamine (100  $\mu$ M) in the absence and in the presence of BFA (20  $\mu$ M, *n* = 7; Fig. 4*C*).

**Histamine Promotes the Growth of Human Subcutaneous Fibroblasts via  $H_1$  Receptor Activation**—Previous reports from the literature demonstrate that histamine promotes fibrosis in a number of different tissues (e.g. lung and skin) by increasing the proliferation of fibroblasts (36, 37), yet the role played by histamine-induced ATP release and subsequent P2 purinoceptor activation in the growth of human subcutaneous fibroblasts has not yet been investigated. Fig. 6*A* (*i*) shows that cultures grown for 28 days in control conditions exhibited a gradual rise in cell viability/proliferation throughout the test period. Results concerning type I collagen production followed a pattern similar to that obtained in the MTT assay (Fig. 6*B*, *i*), indicating that under the present experimental conditions, the amount of extracellular matrix being produced depends directly on the number of viable cells in the culture.

Continuous application of histamine (10–100  $\mu$ M) to the culture medium concentration-dependently increased ( $p < 0.05$ ) human subcutaneous fibroblast proliferation from the first week onward. At days 21 and 28, the MTT reduction values increased ( $p < 0.05$ ) by  $16 \pm 4$  and  $27 \pm 5\%$ , respectively, in the presence of 100  $\mu$ M histamine (*n* = 6), as compared with control values (Fig. 6*A*, *ii*). Histamine (100  $\mu$ M)-induced cells growth was significantly ( $p < 0.05$ ) attenuated in the presence of the selective  $H_1$  receptor antagonist, cetirizine (1  $\mu$ M, *n* = 3). Cetirizine (1  $\mu$ M) *per se* was devoid of a significant ( $p > 0.05$ ) effect (data not shown).

The results concerning type I collagen production are shown in Fig. 6*B* (*ii*). Continuous treatment of the cells with histamine (10–100  $\mu$ M) progressively increased ( $p < 0.05$ ) type I collagen production from the second week onward in a concentration-dependent manner. A maximal increase ( $24 \pm 4\%$ ) of type I collagen production was obtained on day 28 when the cells were incubated with 100  $\mu$ M histamine (*n* = 6) (Fig. 6*B* (*ii*)). Selective blockade of the  $H_1$  receptor with cetirizine (1  $\mu$ M, *n* = 3) significantly ( $p < 0.05$ ) attenuated the increase of type I collagen production caused by histamine (100  $\mu$ M).

Because the amount of type I collagen produced depends on the number of viable cells in the culture (see above), we normalized Sirius Red absorbance values by the corresponding MTT values. This normalization eliminated the differences ( $p > 0.05$ ) from the control situation detected on type I collagen production in the presence of histamine (100  $\mu$ M) (Table 1).

**Histamine-induced Human Fibroblast Growth Is Partially Dependent on P2Y<sub>1</sub> Purinoceptor Activation**—Given that histamine promotes ATP release, we hypothesized that adenine nucleotides could be involved in the proliferative response of human fibroblasts to histamine. Continuous application of ATP (100  $\mu$ M, *n* = 4) and ADP (100  $\mu$ M, *n* = 4) to the culture medium increased ( $p < 0.05$ ) cell growth (MTT assay; Fig. 6*A*, *iii*) and type I collagen production (Sirius Red assay; Fig. 6*B*, *iii*)

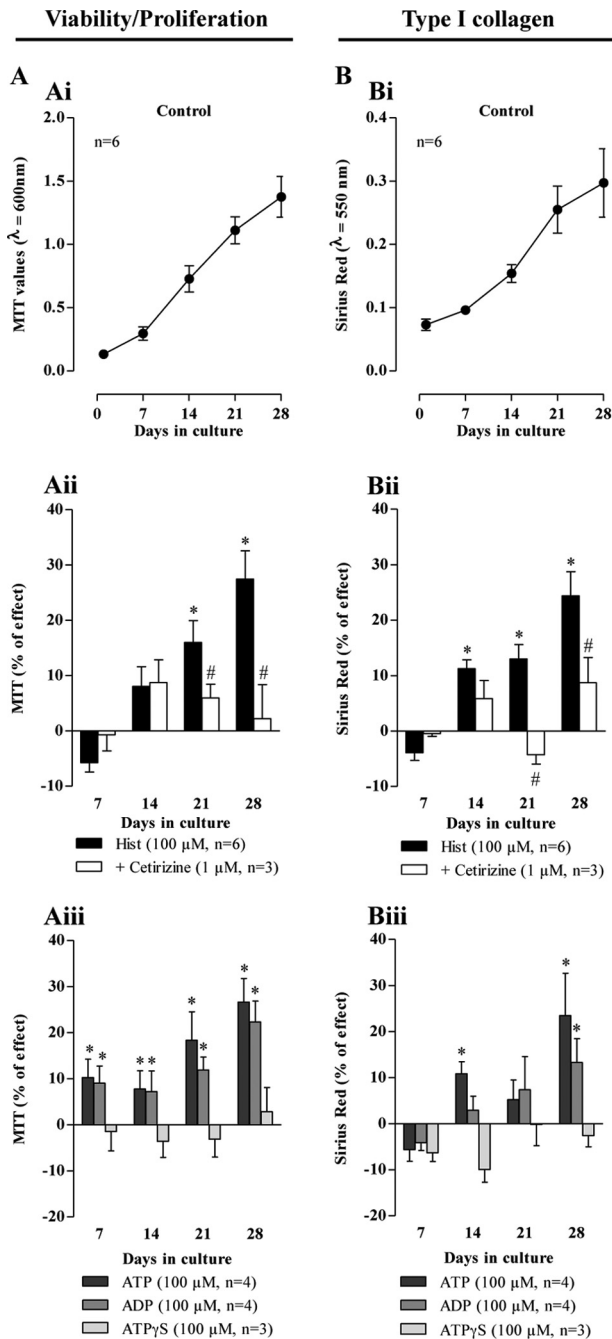


**FIGURE 6. Proliferation/viability and type I collagen production by human subcutaneous fibroblasts grown for 28 days in culture; role of histamine and adenine nucleotides, ATP, ADP, and ATP $\gamma$ S.** *A (i)*, viability/proliferation of cells measured by the MTT assay; results are expressed as absorbance determination at 600 nm/well at certain time points. *B (i)*, total type I collagen production assessed by Sirius Red staining; results are expressed as absorbance determination at 550 nm/well at certain time points. Hist (100  $\mu\text{M}$ ) with or without cetirizine (selective H<sub>1</sub> receptor antagonist; 1  $\mu\text{M}$ ), ATP (100  $\mu\text{M}$ ), ADP (100  $\mu\text{M}$ ), and ATP $\gamma$ S (100  $\mu\text{M}$ ) were all applied continuously to the culture medium. The ordinates represent changes in cell growth (MTT values; *A, ii* and *iii*) and type I collagen production (Sirius Red values; *B, ii* and *iii*) as compared with controls in the absence of test drugs at the same time points (see *A (i)* and *B (i)*). Zero represents similarity between the two values (drug versus control); positive and negative values represent facilitation or inhibition of either cell growth or type I collagen production relative to control data obtained at the same time points. Cetirizine (1  $\mu\text{M}$ ) *per se* was devoid of effect. Each bar represents pooled data from 3–6 individuals; 4–8 replicas were performed for each individual experiment. Vertical bars, S.E. \*,  $p < 0.05$ , significant differences from control values obtained in the absence of tested drugs; #,  $p < 0.05$ , significant differences compared with the effect of Hist (100  $\mu\text{M}$ ) alone.

**TABLE 1**

**Normalization of type I collagen production values to cell growth (MTT assay values) in human subcutaneous fibroblasts grown in culture for 28 days**

Histamine (100  $\mu\text{M}$ ), ATP (100  $\mu\text{M}$ ), and ADP (100  $\mu\text{M}$ ) were added continuously to the culture media of human subcutaneous fibroblasts. Because the amount of type I collagen produced depends on the number of viable cells in culture, we normalized Sirius Red absorbance values by the corresponding MTT values. Values are means  $\pm$  S.E. from 4–6 individuals; 4–8 replicas were performed for each individual experiment. \*,  $p < 0.05$ , significant differences from control values obtained in the absence of tested drugs. n.s., no significance.

| Type I collagen ( $\lambda = 550\text{ nm}$ ) |                           | Type I collagen ( $\lambda = 550\text{ nm}$ ) / MTT values ( $\lambda = 600\text{ nm}$ ) |                           |
|---|---------------------------|--|---------------------------|
| Control                                       | Hist (100 $\mu\text{M}$ ) | Control  | Hist (100 $\mu\text{M}$ ) |
| 0.28 $\pm$ 0.02                               | 0.35 $\pm$ 0.02 (*)       | 0.21 $\pm$ 0.01  | 0.21 $\pm$ 0.01 (n.s.)    |
| Control                                       | ATP (100 $\mu\text{M}$ )  | Control  | ATP (100 $\mu\text{M}$ )  |
| 0.26 $\pm$ 0.02                               | 0.34 $\pm$ 0.03 (*)       | 0.22 $\pm$ 0.02  | 0.22 $\pm$ 0.01 (n.s.)    |
| Control                                       | ADP (100 $\mu\text{M}$ )  | Control  | ADP (100 $\mu\text{M}$ )  |
| 0.26 $\pm$ 0.02                               | 0.31 $\pm$ 0.01 (*)       | 0.22 $\pm$ 0.02  | 0.21 $\pm$ 0.01 (n.s.)    |

by human subcutaneous fibroblasts from the second week onward. The pattern of nucleotide responses was similar to that obtained with histamine (100  $\mu\text{M}$ ) (Fig. 6, *A (ii)* and *B (ii)*, respectively). Normalization of type I collagen production by the content of viable cells also eliminated the differences ( $p > 0.05$ ) from the control situation (Table 1), indicating that (like histamine) adenine nucleotides have a net proliferative effect on human fibroblasts, thereby increasing type I collagen content of the cultures. Interestingly, the enzymatically stable ATP analog, ATP $\gamma$ S (100  $\mu\text{M}$ ,  $n = 3$ ), failed to reproduce the proliferative effect of ATP (100  $\mu\text{M}$ ) (Fig. 6, *A (iii)* and *B (iii)*), thus suggesting that ATP has to be catabolized into ADP in order to promote growth of human subcutaneous fibroblasts.

To investigate the contribution of ADP-sensitive P2Y purinoceptor activation to histamine-induced growth of human subcutaneous fibroblasts, we tested its effect in the presence of selective P2Y<sub>1</sub>, P2Y<sub>12</sub>, and P2Y<sub>13</sub> receptor antagonists (Fig. 7A). Selective blockade of the P2Y<sub>1</sub> receptor with MRS 2179 (0.3  $\mu\text{M}$ ) significantly ( $p < 0.05$ ) attenuated the proliferative action of histamine (100  $\mu\text{M}$ ), but no significant differences ( $p > 0.05$ ) were observed in the presence of AR-C 66096 (0.1  $\mu\text{M}$ ) and MRS 2211 (10  $\mu\text{M}$ ) which selectively antagonize P2Y<sub>12</sub> and P2Y<sub>13</sub> receptors, respectively (Fig. 7A). None of these antagonists modified *per se* human fibroblast proliferation (data not shown).

The presence of ADP-sensitive P2Y purinoceptors in cultured human subcutaneous fibroblasts was confirmed by immunocytochemistry (Fig. 7B) and Western blot (Fig. 7C) analysis. Fluorescence immunoreactivity showed a cytoplasmic/membrane-staining pattern. The P2Y<sub>1</sub> receptor immunoreactivity was the most intense, followed by P2Y<sub>12</sub> and P2Y<sub>13</sub> purinoceptors, which exhibited less significant labeling intensity (Fig. 7B). As illustrated by the Western blots shown in Fig. 7C (*i*), the expected protein bands of human P2Y<sub>1</sub> (63 kDa), P2Y<sub>12</sub> (50 kDa), and P2Y<sub>13</sub> (41 kDa) receptors were detected in homogenates from cultured subcutaneous fibroblasts obtained from all tested individuals (*a, b*, and *c*). The labeling density of ADP-sensitive P2Y receptors normalized to  $\beta$ -tubulin bands indicates that the P2Y<sub>1</sub> is the most expressed receptor in cultured human subcutaneous fibroblasts (Fig. 7C, *ii*).



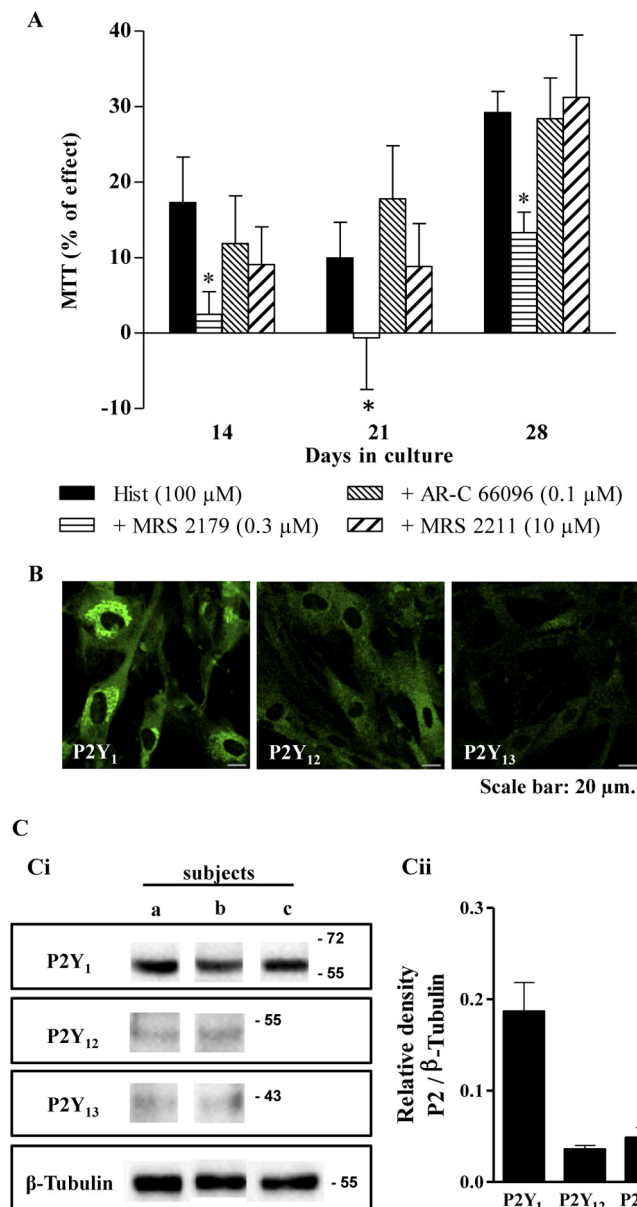


**FIGURE 7. Histamine-induced human fibroblast growth is partially dependent on P2Y<sub>1</sub> purinoceptor activation.** *A*, the variation of cell growth caused by continuous application of Hist (100  $\mu$ M) to the culture medium in the absence and in the presence of selective P2Y<sub>1</sub>, P2Y<sub>12</sub>, and P2Y<sub>13</sub> receptor antagonists: MRS 2179 (0.3  $\mu$ M), AR-C 66096 (0.1  $\mu$ M), and MRS 2211 (10  $\mu$ M), respectively. The ordinates represent changes in MTT values compared with control cultures grown in the absence of test drugs at the same time points (see Fig. 4). Zero represents similarity between the two values (drug versus control); positive and negative values represent facilitation or inhibition of cell growth relative to the control situation at the same time points. Each bar represents pooled data from two individuals; four replicates were performed for each individual experiment. Vertical bars, S.E. \*,  $p < 0.05$ , significant differences compared with the effect of Hist (100  $\mu$ M) alone. *B*, immunoreactivity of human subcutaneous fibroblasts against P2Y<sub>1</sub>, P2Y<sub>12</sub>, and P2Y<sub>13</sub> receptors at culture day 7. Images were obtained under a confocal microscope. Results are representative of three independent experiments. Scale bar, 20  $\mu$ m. *C* (i), representative immunoblots of P2Y<sub>1</sub>, P2Y<sub>12</sub>, and P2Y<sub>13</sub> receptor expression in cultured human subcutaneous fibroblasts from three distinct individuals (a, b, and c). *C* (ii), quantification of P2Y<sub>1</sub>, P2Y<sub>12</sub>, and P2Y<sub>13</sub> receptor levels using  $\beta$ -tubulin as a reference protein of experiments shown in *C* (i).

*Pattern of the Extracellular Catabolism of Adenine Nucleotides in Human Subcutaneous Fibroblast Cultures*—Fig. 8 illustrates the time course of the extracellular catabolism of adenine

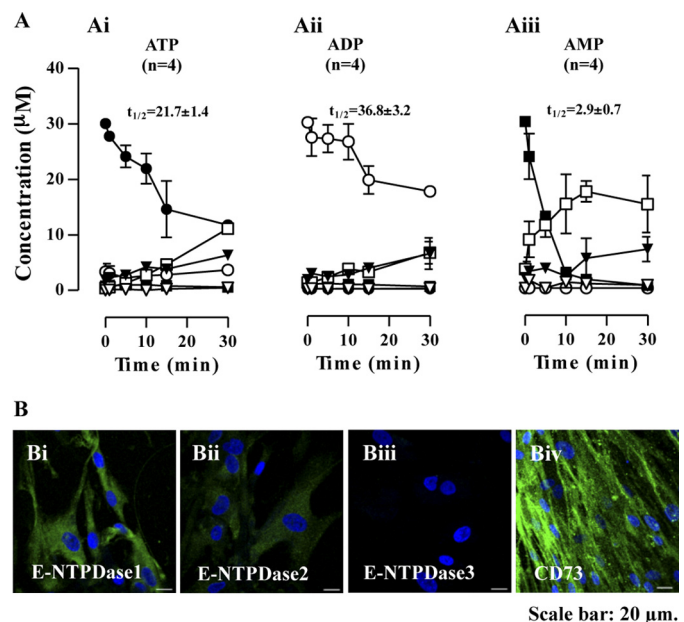


**FIGURE 8. Time course of the extracellular catabolism of adenine nucleotides and immunocytochemical detection of E-NTPDases in human subcutaneous fibroblast cultures at day 11.** ATP (*A*, i), ADP (*A*, ii), and AMP (*A*, iii) were added at a concentration of 30  $\mu$ M to the culture medium at time 0. Samples (75  $\mu$ l) were collected from each well at the times indicated on the abscissa. Each collected sample was analyzed by HPLC to separate and quantify ATP (filled circles), ADP (open circles), AMP (filled squares), adenosine (open squares), inosine (filled triangles), or hypoxanthine (open triangles). Each point represents pooled data from two individuals; two replicates were performed in each individual experiment. Vertical bars, S.E., shown when they exceed the symbols in size. The calculated half-life time ( $t_{1/2}$ , min) for each initial substrate is shown for comparison. *B*, immunoreactivity of human subcutaneous fibroblasts against E-NTPDase1, E-NTPDase2, E-NTPDase3, and E-5'-nucleotidase (CD73). Cells grown in 8-well chamber slides were processed for immunocytochemistry in parallel and were visualized, keeping unaltered the settings of the confocal microscope throughout the procedure. Scale bar, 20  $\mu$ m.

nucleotides, ATP, ADP, and AMP, in the first subculture of fibroblasts isolated from the human subcutaneous tissue. ATP (30  $\mu$ M) was metabolized with a half-life time of  $21.7 \pm 1.4$  min ( $n = 4$  observations from two individuals). The ATP metabolites detected in the bath were ADP, adenosine, and inosine, whose concentrations increased progressively with time, reaching maximal values of  $3.7 \pm 0.7$ ,  $11.1 \pm 0.8$ , and  $6.3 \pm 0.5$   $\mu$ M, respectively, 30 min after ATP (30  $\mu$ M) application (Fig. 8*A*, i). The extracellular catabolism of ADP (30  $\mu$ M) was significantly ( $p < 0.05$ ) slower (half-life time of  $36.8 \pm 3.2$  min,  $n = 4$  observations from two individuals) than that of ATP (30  $\mu$ M). ADP was metabolized into adenosine and inosine, whose concentrations increased with time, reaching maximal values of  $6.6 \pm 1.7$  and  $6.4 \pm 2.3$   $\mu$ M, respectively, 30 min after ADP (30  $\mu$ M) application (Fig. 8*A*, ii). Interestingly, AMP (30  $\mu$ M) was almost completely dephosphorylated into adenosine and inosine with a half-life time of  $2.9 \pm 0.7$  min ( $n = 4$  observations from two individuals), which might explain why the accumulation of AMP was almost negligible (less than 1  $\mu$ M) when ATP (30  $\mu$ M) and ADP (30  $\mu$ M) were used as substrates (Fig. 8*A*, iii).

Given the linearity of the semilogarithmic representation of progress curves obtained by polynomial fitting of the catabolism of ATP ( $y = -0.0134x + 1.3631$ ,  $R^2 = 0.9334$ ), ADP ( $y = -0.0078x + 1.4118$ ,  $R^2 = 0.8850$ ), and AMP ( $y = -0.0610x + 1.2594$ ,  $R^2 = 0.9096$ ), the analysis of the corresponding half-life

time values clearly indicates that the extracellular catabolism of ATP/ADP into AMP through E-NTPDases is the rate-limiting step to generate adenosine from exogenously added adenine nucleotides, as we previously observed in human bone marrow stromal cells (11, 18).

The expression of E-NTPDase family members 1, 2, and 3 and of E-5'-nucleotidase (also called CD73, EC 3.1.3.5) was assessed by immunofluorescence confocal microscopy (Fig. 8B). Human subcutaneous fibroblasts exhibited a strong immunoreactivity against E-5'-nucleotidase (Fig. 8B, *iv*), thus supporting the high AMP dephosphorylation rate detected in the enzymatic kinetic studies (Fig. 8A, *iii*). These cells also stained positively for E-NTPDase1 (also called CD39 or apyrase, EC 3.6.1.5) (Fig. 8B, *i*) as well as for E-NTPDase2 (CD39L1, EC 3.6.1.3) (Fig. 8B, *ii*), although for the latter, the immunoreactivity was less intense. No immunoreactivity against E-NTPDase3 (CD39L3 or HB6) was detected in these cells (Fig. 8B, *iii*).

## DISCUSSION

Histamine belongs to a group of endogenous chemical substances that are released upon cell damage or during inflammatory insults (38–40). The role of histamine in nociception is not clear, but it appears to cooperate with the effect of other endogenous mediators (41). It has been shown that histamine, together with substance P, is capable of inducing ATP release from smooth muscle cells of the guinea pig vas deferens (12). To the best of our knowledge, this is the first study demonstrating that human fibroblasts isolated from subcutaneous connective tissue respond to histamine by releasing ATP into the extracellular media through the activation of  $H_1$  receptors.

Results also showed that histamine triggers intracellular  $Ca^{2+}$  mobilization via the activation of  $G_q$  protein-coupled  $H_1$  receptors, given that inhibition of phospholipase C with U73122 and depletion of intracellular  $Ca^{2+}$  stores caused by thapsigargin attenuated its response. Moreover, extracellular  $Ca^{2+}$  might also play some role to sustain the late component of histamine-induced  $[Ca^{2+}]_i$  rise, because its removal from the incubation medium significantly attenuated histamine response. A similar response to histamine has been reported in epithelial cells (42). Our findings could be explained by a possible involvement of store-operated calcium channels in order to compensate for the fall of the  $[Ca^{2+}]_i$  content (43) and/or through a concurrent activation of other membrane receptors, namely P2 purinoceptors. Attenuation of histamine-induced  $[Ca^{2+}]_i$  response by apyrase suggests cooperation with a nucleotide mediator, such as ATP and/or ADP. Because blockade of P2 purinoceptors mimicked the attenuating effect of apyrase, our data provide the first evidence that histamine-induced  $[Ca^{2+}]_i$  accumulation by fibroblasts of human subcutaneous tissue is partially mediated by the release of ATP and subsequent activation of P2 purinoceptors. Recently, it was demonstrated that stretch-induced ATP release in rat subcutaneous fibroblasts influences cytoskeletal remodeling of the cells in part by the subsequent activation of P2 purinoceptors (44).

Depending on the cell type, there are multiple nucleotide-releasing pathways, which represent a critical component for the initiation of the purinergic signaling cascade (13). Considering that  $Ca^{2+}$  signaling induced by histamine seems to par-

tially involve P2 purinoceptor activation subsequent to the release of ATP from fibroblasts of the human subcutaneous tissue, we assessed the contribution of several nucleotide-releasing mechanisms by measuring  $[Ca^{2+}]_i$  oscillations. Histamine-induced  $[Ca^{2+}]_i$  oscillations were not affected upon inhibition of the vesicular transport with BFA, thus suggesting that exocytosis might not represent an important pathway for releasing ATP in these cells. Further studies designed to investigate unloading of vesicular ATP stores stained with quinacrine are required to exclude this possibility in human fibroblasts (45). Here, we proved that human subcutaneous fibroblasts express Cx43 and Panx1 hemichannels. Although both channels have been committed to translocation of nucleotides to the extracellular milieu in numerous cell types, functional data using non-selective connexin inhibitors, such as 2-octanol and MFQ, failed to modify histamine-induced  $[Ca^{2+}]_i$  oscillations in fibroblasts of the human subcutaneous tissue. Conversely, blockade of Panx1-containing hemichannels with CBX (32),  $^{10}Panx$  (33), and probenecid (34) significantly attenuated the histamine-induced  $[Ca^{2+}]_i$  response. Given that probenecid is a powerful Panx1 inhibitor with no effect on connexin channels, our findings suggest that Panx1-containing hemichannels might have a predominant role in histamine-induced  $[Ca^{2+}]_i$  responses operated by ATP released from human subcutaneous fibroblasts. The reason for the disparity between protein expression and function may be that Cx43, unlike Panx1, hemichannels close at normal millimolar  $Ca^{2+}$  (e.g. 1.8 mM  $CaCl_2$  in Tyrode's solution) and open upon external  $Ca^{2+}$  depletion (46).

The involvement of ATP-releasing hemichannels was further confirmed by time-lapse fluorescence microscopy demonstrating the uptake of To-Pro3 by cultured human fibroblasts. Following the initial  $[Ca^{2+}]_i$  peak, histamine caused a sustained increase in To-Pro3 dye uptake by the cells, which paralleled the second component of  $[Ca^{2+}]_i$  rise. Sustained effects of histamine on both  $[Ca^{2+}]_i$  and To-Pro3 dye uptake were significantly attenuated upon blocking pannexin-1 hemichannel permeability with CBX and H1152, thus implicating the opening of large membrane pores that facilitate translocation of high molecular mass molecules (like ATP) between intra- and extracellular compartments.

The molecular mechanism(s) by which histamine releases ATP through the opening of Panx1 hemichannels in human subcutaneous fibroblasts deserves further investigation. Nevertheless, disregarding whether channel-mediated efflux or vesicle exocytosis comprises the predominant ATP release mechanism, most studies have identified elevation of cytosolic  $Ca^{2+}$  as an important regulator of ATP release in different cell models. Generation of inositol trisphosphate by phospholipase C may be the process underlying elevation of cytosolic  $Ca^{2+}$  (47, 48). Histamine  $H_1$  receptor, like other  $G_q$ -coupled receptors, may additionally stimulate Rho-GTPase (via  $G_{12/13}$ ), acting to strongly potentiate the  $Ca^{2+}$ -activated ATP release pathway (49, 50). Rho activation and  $Ca^{2+}$  mobilization must be temporally coordinated to promote ATP release. Interestingly, Seminario-Vidal *et al.* (50) demonstrated that  $Ca^{2+}$ - and RhoA/Rho kinase-dependent ATP release from thrombin-stimulated A549 lung epithelial cells occurs via connexin or pannexin

hemichannels, but this pathway might not be competent for ATP release in human astrocytoma cells (49). Given the actions exerted by Rho/Rho kinase on scaffold proteins and cytoskeleton components (e.g. regulating myosin light chain phosphorylation and actin polymerization), the authors speculate that Rho-promoted membrane-cytoskeleton rearrangements facilitate the insertion of hemichannel subunits within the plasma membrane. Blockade of one of these multiple mechanisms might explain the attenuating effect of the Rho kinase inhibitor H1152 on histamine-induced  $[Ca^{2+}]_i$  rise observed in this study. These findings suggest that RhoA/Rho kinase activation is a step upstream of Panx1-mediated ATP release triggered by histamine in human subcutaneous fibroblasts.

Our data also demonstrate that fibroblasts of human subcutaneous connective tissue respond to histamine by increasing cell growth and subsequent type I collagen production through the activation of  $H_1$  receptors. Normalization of type I collagen production by the number of viable cells indicates that histamine exerts a preferential effect on cell proliferation rather than in extracellular matrix remodeling. In lungs and skin, histamine exerts a profibrotic action by increasing cells growth (36, 37) and collagen deposition (37, 51) via  $H_2$  receptor activation. Despite the close anatomical proximity between skin and subcutaneous connective tissue, functional differences between fibroblasts from different tissue origins have been described (52, 53). Thus, differences between our findings and previous reports regarding the receptor subtype involved in the action of histamine may be explained by differences in tissue and species origin. On the other hand, distinct methodological approaches have been used. Previous studies (36, 37, 51) exposed cells to histamine from several hours to a few days (7 days), whereas we monitored histamine-induced effects in cells kept in culture for 28 days. Moreover, in contrast to previous studies, we found significant differences in cell growth and type I collagen production induced by histamine (10–100  $\mu M$ ) exposure from the second week onward. Actually, we did not monitor acute (for hours to a few days) changes operated by histamine in our cultures. These findings strengthen the idea that, although fibroblasts are ubiquitous mesenchymal cells, they may function differently depending on their location.

Given that histamine triggered the release of ATP from human subcutaneous fibroblasts in culture, we postulated that adenine nucleotides could be involved in the proliferative response of histamine in these cells. Continuous application of ATP and ADP to the culture medium mimicked the proliferative effect of histamine, indicating that adenine nucleotides promote human fibroblast growth and subsequent type I collagen production. Surprisingly, no such effect was found with the enzymatically stable ATP analog, ATP $\gamma$ S. Thus, it seems that cells exposed to histamine release ATP into the extracellular milieu, which, upon conversion into ADP, indirectly promotes growth of human subcutaneous fibroblasts. In fact, selective blockade of ADP-sensitive  $P2Y_1$  receptors attenuated histamine-induced cell proliferation, but no changes were detected in the presence of the selective  $P2Y_{12}$  and  $P2Y_{13}$  antagonists. The presence of  $P2Y_1$  receptors in fibroblasts of the human subcutaneous tissue was confirmed by immunofluorescence confocal microscopy and Western blot analysis. Data show that

immunoreactivity against the  $P2Y_1$  receptor was much more intense as compared with that of  $P2Y_{12}$  and  $P2Y_{13}$  receptors. Functional data and immunolabeling experiments are consistent with ADP-sensitive  $P2Y_1$  being the receptor subtype mediating the purinergic loop leading to cell growth in response to histamine. This outcome is particularly interesting considering that the  $P2Y_1$  receptor, along with the  $P2Y_2$  and  $P2X_7$  subtypes, has been implicated in chronic inflammation (10). These authors used disks made of non-cytotoxic degradable dermal sheep collagen implanted subcutaneously in rats to monitor the foreign body inflammatory reaction for 21 days. They found that  $P2Y_1$ ,  $P2Y_2$ , and  $P2X_7$  receptors were up-regulated, in parallel to vascular activation and increased number of macrophages and giant cells. Although fibroblasts were shown to encapsulate the disks and to promote deposition of extracellular matrix components (10), these cells were not further evaluated. Given that inflammatory reactions involve the recruitment of mast cells, which release huge amounts of histamine to the extracellular milieu, we speculate that activated fibroblasts would proliferate, thus contributing to the global increase in  $P2Y_1$  receptor expression.

The activity of ecto-nucleotidases is critical to define the inactivation rate of adenine nucleotides within close proximity of the release sites in tissue microenvironments. In this study, we analyzed the role of three members of the ecto-nucleoside triphosphate diphosphohydrolase (E-NTPDase) family, namely E-NTPDase1, E-NTPDase2, and E-NTPDase3 (54). These enzymes have distinct biochemical properties. E-NTPDase1 hydrolyzes ATP and ADP equally well, E-NTPDase2 preferentially hydrolyzes triphosphonucleosides, and E-NTPDase3 has an intermediate hydrolysis profile (55). The hydrolysis of tri- and diphosphonucleosides by E-NTPDases yields AMP as the final product, which can be fully dephosphorylated to adenosine by E-5'-nucleotidase/CD73 (56). Our results showed that human subcutaneous fibroblasts exhibit a strong immunoreactivity against E-5'-nucleotidase/CD73, which is in keeping with a faster conversion of AMP into adenosine. A high E-5'-nucleotidase/CD73 activity might also explain why the concentration of AMP was kept at a low level when ATP and/or ADP were used as substrates (57).

Luttikhuisen *et al.* (10) reported the overexpression of subcutaneous E-NTPDase1 in a model of chronic inflammation. Interestingly, we showed here that human subcutaneous fibroblasts express E-NTPDase1 immunoreactivity under resting conditions. This member of the NTPDase family seems to be the most expressed ATP- and/or ADP-metabolizing enzyme in these cells, as predicted from lesser immunofluorescence signals obtained for other E-NTPDases. These cells exhibit weak immunoreactivity against E-NTPDase2, and no signal was detected for E-NTPDase3, suggesting that E-NTPDase2 may participate together with E-NTPDase1 in the extracellular catabolism of adenine nucleotides in fibroblasts of the human subcutaneous tissue. E-NTPDase1, E-NTPDase2, and E-NTPDase3 hydrolyze extracellular tri- and diphosphonucleotides with ATP/ADP ratios of  $\sim 1$ – $2$ : $1$ ,  $\sim 10$ – $40$ : $1$ , and  $\sim 3$ – $4$ : $1$ , respectively (55). The kinetic analysis of the extracellular catabolism of ATP and ADP in human subcutaneous fibroblast cultures indicates that adenine nucleotides are metabolized



with a ratio of  $\sim 1.5(\text{ATP}):1(\text{ADP})$ , which is compatible with E-NTPDase1 being the most effective isoform in these cultures. In line with this hypothesis, one would expect that the formation of adenosine should be prevented if NTPDase2 acted alone, or it could be delayed if NTPDase3 was the main enzyme involved in the catabolism of adenine nucleotides, given that it is well known that E-5'-nucleotidase/CD73 is inhibited by ADP (55, 57). Our results proved exactly the opposite, showing that AMP was rapidly dephosphorylated into adenosine independently of the nucleotide substrate used. On the other hand, involvement of E-NTPDase1 is expected to terminate the effects exerted by either ATP- or ADP-sensitive receptors. Nevertheless, data indicate that responses of human subcutaneous fibroblasts to histamine depend on the activation of ADP-sensitive P2Y<sub>1</sub> receptors. This situation can occur because E-NTPDase2 concurs with E-NTPDase1 to release enough ADP required to activate P2Y<sub>1</sub> receptors in human subcutaneous fibroblasts, because the former enzyme preferentially hydrolyzes triphosphonucleosides.

In conclusion, our findings showed for the first time that histamine promotes the release of ATP from human subcutaneous fibroblasts via Panx1 hemichannels, leading to  $[\text{Ca}^{2+}]_i$  mobilization from internal stores and cell growth through the cooperation of H<sub>1</sub> and P2Y receptors (most probably of the P2Y<sub>1</sub> subtype) activation. Targeting the pathways leading to nucleotide release and the purinergic cascade, consisting in metabolizing E-NTPDase and P2 purinoceptor activation, may be useful in designing novel therapies toward the modulation of cell signals between fibroblasts, nociceptors, and inflammatory cells, which underlie the pathogenesis of painful musculoskeletal diseases with widespread involvement of the subcutaneous connective tissue, such as fibromyalgia.

**Acknowledgments**—We especially thank Professor J. M. LaFuente-de-Carvalho (Serviço de Urologia, Centro Hospitalar do Porto (CHP), Porto, Portugal) for providing the human tissue samples required for fibroblasts isolation. We acknowledge Julie Pelletier and Dr. Joanna Lecka for assistance in the generation of NTPDase antibodies, Dr. Catarina Moreira for collaboration in HPLC analysis, and Dr. Sónia Gomes for assistance in Western blot experiments. We also thank M. Helena Costa e Silva and Belmira Silva for technical assistance.

## REFERENCES

- Langevin, H. M., Cornbrooks, C. J., and Taatjes, D. J. (2004) Fibroblasts form a body-wide cellular network. *Histochem. Cell Biol.* **122**, 7–15
- Hedley, G. (2008) Demonstration of the integrity of human superficial fascia as an autonomous organ. *J. Bodyw. Mov. Ther.* **12**, 258
- Langevin, H. M., and Sherman, K. J. (2007) Pathophysiological model for chronic low back pain integrating connective tissue and nervous system mechanisms. *Med. Hypotheses* **68**, 74–80
- Langevin, H. M., Stevens-Tuttle, D., Fox, J. R., Badger, G. J., Bouffard, N. A., Krag, M. H., Wu, J., and Henry, S. M. (2009) Ultrasound evidence of altered lumbar connective tissue structure in human subjects with chronic low back pain. *BMC Musculoskelet. Disord.* **10**, 151
- Willis, W. D. C., R. E. (1991) *Sensory Mechanisms of the Spinal Cord*, 2nd Ed., Plenum Press, New York
- Corey, S. M., Vizzard, M. A., Badger, G. J., and Langevin, H. M. (2011) Sensory innervation of the nonspecialized connective tissues in the low back of the rat. *Cells Tissues Organs* **194**, 521–530
- Ansel, J. C., Kaynard, A. H., Armstrong, C. A., Olerud, J., Bunnett, N., and Payan, D. (1996) Skin-nervous system interactions. *The J. Invest. Dermatol.* **106**, 198–204
- Katayama, I., and Nishioka, K. (1997) Substance P augments fibrogenic cytokine-induced fibroblast proliferation. Possible involvement of neuro-peptide in tissue fibrosis. *J. Dermatol. Sci.* **15**, 201–206
- Dray, A. (1995) Inflammatory mediators of pain. *Br. J. Anaesth.* **75**, 125–131
- Luttikhuisen, D. T., Harmsen, M. C., de Leij, L. F., and van Luyn, M. J. (2004) Expression of P2 receptors at sites of chronic inflammation. *Cell Tissue Res.* **317**, 289–298
- Noronha-Matos, J. B., Costa, M. A., Magalhães-Cardoso, M. T., Ferreirinha, F., Pelletier, J., Freitas, R., Neves, J. M., Sévigny, J., and Correia-de-Sá, P. (2012) Role of ecto-NTPDases on UDP-sensitive P2Y<sub>6</sub> receptor activation during osteogenic differentiation of primary bone marrow stromal cells from postmenopausal women. *J. Cell. Physiol.* **227**, 2694–2709
- Tamesue, S., Sato, C., and Katsuragi, T. (1998) ATP release caused by bradykinin, substance P and histamine from intact and cultured smooth muscles of guinea-pig vas deferens. *Naunyn Schmiedeberg's Arch. Pharmacol.* **357**, 240–244
- Yegutkin, G. G. (2008) Nucleotide- and nucleoside-converting ectoenzymes. Important modulators of purinergic signalling cascade. *Biochim. Biophys. Acta* **1783**, 673–694
- Faria, M., Magalhães-Cardoso, T., Lafuente-de-Carvalho, J. M., and Correia-de-Sá, P. (2006) Corpus cavernosum from men with vasculogenic impotence is partially resistant to adenosine relaxation due to endothelial A<sub>2B</sub> receptor dysfunction. *J. Pharmacol. Exp. Ther.* **319**, 405–413
- Orriss, I. R., Knight, G. E., Ranasinghe, S., Burnstock, G., and Arnett, T. R. (2006) Osteoblast responses to nucleotides increase during differentiation. *Bone* **39**, 300–309
- Henriksen, Z., Hiken, J. F., Steinberg, T. H., and Jørgensen, N. R. (2006) The predominant mechanism of intercellular calcium wave propagation changes during long-term culture of human osteoblast-like cells. *Cell calcium* **39**, 435–444
- Panupinhu, N., Zhao, L., Possmayer, F., Ke, H. Z., Sims, S. M., and Dixon, S. J. (2007) P2X7 nucleotide receptors mediate blebbing in osteoblasts through a pathway involving lysophosphatidic acid. *J. Biol. Chem.* **282**, 3403–3412
- Costa, M. A., Barbosa, A., Neto, E., Sá-e-Sousa, A., Freitas, R., Neves, J. M., Magalhães-Cardoso, T., Ferreirinha, F., and Correia-de-Sá, P. (2011) On the role of subtype selective adenosine receptor agonists during proliferation and osteogenic differentiation of human primary bone marrow stromal cells. *J. Cell. Physiol.* **226**, 1353–1366
- Tullberg-Reinert, H., and Jundt, G. (1999) *In situ* measurement of collagen synthesis by human bone cells with a sirius red-based colorimetric microassay. Effects of transforming growth factor  $\beta$ 2 and ascorbic acid 2-phosphate. *Histochem. Cell Biol.* **112**, 271–276
- Magalhães-Cardoso, M. T., Pereira, M. F., Oliveira, L., Ribeiro, J. A., Cunha, R. A., and Correia-de-Sá, P. (2003) Ecto-AMP deaminase blunts the ATP-derived adenosine A<sub>2A</sub> receptor facilitation of acetylcholine release at rat motor nerve endings. *J. Physiol.* **549**, 399–408
- Cunha, R. A., Sebastião, A. M., and Ribeiro, J. A. (1998) Inhibition by ATP of hippocampal synaptic transmission requires localized extracellular catabolism by ecto-nucleotidases into adenosine and channeling to adenosine A<sub>1</sub> receptors. *J. Neurosci.* **18**, 1987–1995
- Dranoff, J. A., Kruglov, E. A., Toure, J., Braun, N., Zimmermann, H., Jain, D., Knowles, A. F., and Sévigny, J. (2004) Ectonucleotidase NTPDase2 is selectively down-regulated in biliary cirrhosis. *J. Investig. Med.* **52**, 475–482
- Munkonda, M. N., Pelletier, J., Ivanenkov, V. V., Fausther, M., Tremblay, A., Künzli, B., Kirley, T. L., and Sévigny, J. (2009) Characterization of a monoclonal antibody as the first specific inhibitor of human NTP diphosphohydrolase-3. Partial characterization of the inhibitory epitope and potential applications. *FEBS J.* **276**, 479–496
- Alqallaf, S. M., Evans, B. A., and Kidd, E. J. (2009) Atypical P2X receptor pharmacology in two human osteoblast-like cell lines. *Br. J. Pharmacol.* **156**, 1124–1135
- Freshney, R. I. (2000) *Culture of Animal Cells: A Manual of Basic Technique*, 4th Ed., Wiley-Liss, New York
- Gartner, L. P., and Hiatt, J. L. (2007) *Color Textbook of Histology*, 3rd Ed.,

27. Agocha, A. E., and Eghbali-Webb, M. (1997) A simple method for preparation of cultured cardiac fibroblasts from adult human ventricular tissue. *Mol. Cell. Biochem.* **172**, 195–198
28. Thastrup, O., Cullen, P. J., Drøbak, B. K., Hanley, M. R., and Dawson, A. P. (1990) Thapsigargin, a tumor promoter, discharges intracellular  $\text{Ca}^{2+}$  stores by specific inhibition of the endoplasmic reticulum  $\text{Ca}^{2+}$ -ATPase. *Proc. Natl. Acad. Sci. U.S.A.* **87**, 2466–2470
29. Asazuma-Nakamura, Y., Dai, P., Harada, Y., Jiang, Y., Hamaoka, K., and Takamatsu, T. (2009) Cx43 contributes to TGF- $\beta$  signaling to regulate differentiation of cardiac fibroblasts into myofibroblasts. *Exp. Cell Res.* **315**, 1190–1199
30. Cruikshank, S. J., Hopperstad, M., Younger, M., Connors, B. W., Spray, D. C., and Srinivas, M. (2004) Potent block of Cx36 and Cx50 gap junction channels by mefloquine. *Proc. Natl. Acad. Sci. U.S.A.* **101**, 12364–12369
31. Juszczak, G. R., and Swiergiel, A. H. (2009) Properties of gap junction blockers and their behavioural, cognitive and electrophysiological effects. Animal and human studies. *Prog. Neuropsychopharmacol. Biol. Psychiatry* **33**, 181–198
32. D'hondt, C., Ponsaerts, R., De Smedt, H., Bultynck, G., and Himpens, B. (2009) Pannexins, distant relatives of the connexin family with specific cellular functions? *BioEssays* **31**, 953–974
33. Wang, J., Ma, M., Locovei, S., Keane, R. W., and Dahl, G. (2007) Modulation of membrane channel currents by gap junction protein mimetic peptides. Size matters. *Am. J. Physiol. Cell Physiol.* **293**, C1112–C1119
34. Silverman, W., Locovei, S., and Dahl, G. (2008) Probenecid, a gout remedy, inhibits pannexin 1 channels. *Am. J. Physiol. Cell Physiol.* **295**, C761–C767
35. Chekeni, F. B., Elliott, M. R., Sandilos, J. K., Walk, S. F., Kinchen, J. M., Lazarowski, E. R., Armstrong, A. J., Penuela, S., Laird, D. W., Salvesen, G. S., Isakson, B. E., Bayliss, D. A., and Ravichandran, K. S. (2010) Pannexin 1 channels mediate “find-me” signal release and membrane permeability during apoptosis. *Nature* **467**, 863–867
36. Jordana, M., Befus, A. D., Newhouse, M. T., Bienenstock, J., and Gauldie, J. (1988) Effect of histamine on proliferation of normal human adult lung fibroblasts. *Thorax* **43**, 552–558
37. Garbuzenko, E., Nagler, A., Pickholtz, D., Gillery, P., Reich, R., Maquart, F. X., and Levi-Schaffer, F. (2002) Human mast cells stimulate fibroblast proliferation, collagen synthesis and lattice contraction. A direct role for mast cells in skin fibrosis. *Clin. Exp. Allergy* **32**, 237–246
38. Pleuvry, B. J., and Lauretti, G. R. (1996) Biochemical aspects of chronic pain and its relationship to treatment. *Pharmacol. Ther.* **71**, 313–324
39. Besson, J. M. (1999) The neurobiology of pain. *Lancet* **353**, 1610–1615
40. Mørk, H., Ashina, M., Bendtsen, L., Olesen, J., and Jensen, R. (2003) Experimental muscle pain and tenderness following infusion of endogenous substances in humans. *Eur. J. Pain* **7**, 145–153
41. Markenson, J. A. (1996) Mechanisms of chronic pain. *Am. J. Med.* **101**, 6S–18S
42. Riach, R. A., Duncan, G., Williams, M. R., and Webb, S. F. (1995) Histamine and ATP mobilize calcium by activation of H1 and P2u receptors in human lens epithelial cells. *J. Physiol.* **486**, 273–282
43. Parekh, A. B., and Putney, J. W., Jr. (2005) Store-operated calcium channels. *Physiol. Rev.* **85**, 757–810
44. Langevin, H. M., Fujita, T., Bouffard, N. A., Takano, T., Koptiuch, C., Badger, G. J., and Nedergaard, M. (2013) Fibroblast cytoskeletal remodeling induced by tissue stretch involves ATP signaling. *J. Cell. Physiol.* **228**, 1922–1926
45. Bodin, P., and Burnstock, G. (2001) Evidence that release of adenosine triphosphate from endothelial cells during increased shear stress is vesicular. *J. Cardiovasc. Pharmacol.* **38**, 900–908
46. Fasciani, I., Temperan, A., Perez-Atencio, L. F., Escudero, A., Martinez-Montero, P., Molano, J., Gomez-Hernandez, J. M., Paino, C. L., Gonzalez-Nieto, D., and Barrio, L. C. (2013) Regulation of connexin hemichannel activity by membrane potential and the extracellular calcium in health and disease. *Neuropharmacology* 10.1016/j.neuropharm.2013.03.040
47. De Vuyst, E., Decrock, E., Cabooter, L., Dubyak, G. R., Naus, C. C., Evans, W. H., and Leybaert, L. (2006) Intracellular calcium changes trigger connexin 32 hemichannel opening. *EMBO J.* **25**, 34–44
48. Iglesias, R., Dahl, G., Qiu, F., Spray, D. C., and Scemes, E. (2009) Pannexin 1. The molecular substrate of astrocyte “hemichannels”. *J. Neurosci.* **29**, 7092–7097
49. Blum, A. E., Joseph, S. M., Przybylski, R. J., and Dubyak, G. R. (2008) Rho-family GTPases modulate  $\text{Ca}^{2+}$ -dependent ATP release from astrocytes. *Am. J. Physiol. Cell Physiol.* **295**, C231–C241
50. Seminario-Vidal, L., Kreda, S., Jones, L., O’Neal, W., Trejo, J., Boucher, R. C., and Lazarowski, E. R. (2009) Thrombin promotes release of ATP from lung epithelial cells through coordinated activation of Rho- and  $\text{Ca}^{2+}$ -dependent signaling pathways. *J. Biol. Chem.* **284**, 20638–20648
51. Hatamochi, A., Fujiwara, K., and Ueki, H. (1985) Effects of histamine on collagen synthesis by cultured fibroblasts derived from guinea pig skin. *Arch. Dermatol. Res.* **277**, 60–64
52. Chang, H. Y., Chi, J. T., Dudoit, S., Bondre, C., van de Rijn, M., Botstein, D., and Brown, P. O. (2002) Diversity, topographic differentiation, and positional memory in human fibroblasts. *Proc. Natl. Acad. Sci. U. S. A.* **99**, 12877–12882
53. Rinn, J. L., Bondre, C., Gladstone, H. B., Brown, P. O., and Chang, H. Y. (2006) Anatomic demarcation by positional variation in fibroblast gene expression programs. *PLoS Genet.* **2**, e119
54. Robson, S. C., Sévigny, J., and Zimmermann, H. (2006) The E-NTPDase family of ectonucleotidases. Structure function relationships and pathophysiological significance. *Purinergic Signal.* **2**, 409–430
55. Kukulski, F., Lévesque, S. A., Lavoie, E. G., Lecka, J., Bigonnesse, F., Knowles, A. F., Robson, S. C., Kirley, T. L., and Sévigny, J. (2005) Comparative hydrolysis of P2 receptor agonists by NTPDases 1, 2, 3 and 8. *Purinergic Signal.* **1**, 193–204
56. Colgan, S. P., Eltzschig, H. K., Eckle, T., and Thompson, L. F. (2006) Physiological roles for ecto-5'-nucleotidase (CD73). *Purinergic Signal.* **2**, 351–360
57. Fausther, M., Lecka, J., Soliman, E., Kauffenstein, G., Pelletier, J., Sheung, N., Dranoff, J. A., and Sévigny, J. (2012) Coexpression of ecto-5'-nucleotidase/CD73 with specific NTPDases differentially regulates adenosine formation in the rat liver. *Am. J. Physiol. Gastrointest. Liver Physiol.* **302**, G447–G459

\* This work was supported in part by Fundação para a Ciência e a Tecnologia (Fundo Europeu de Desenvolvimento Regional, FEDER) Grant PTDC/SAU-FCF/108263/2008 and by grants from the Canadian Institutes of Health Research and from the Arthritis Society (to J. S.).

<sup>1</sup> Recipient of Fundação para a Ciência e a Tecnologia Ph.D. Scholarship SFRH/BD/47373/2008.

<sup>2</sup> Recipient of a Chercheur Boursier Senior from the Fonds de Recherche Santé-Québec.

<sup>3</sup> To whom correspondence should be addressed: Laboratório de Farmacologia e Neurobiologia, Unidade Multidisciplinar de Investigação Biomédica, Instituto de Ciências Biomédicas de Abel Salazar-Universidade do Porto, Rua Jorge Viterbo Ferreira 228, Edif. 2 Piso 4, 4050-313 Porto, Portugal. Tel.: 351-220-428-212; Fax: 351-220-428-090; E-mail: farmacol@icbas.up.pt.